Center Determination for Cone-Beam X-ray Tomography

W. Narkbuakaew, S. Ngamanekrat*, W. Withayachumnankul, C. Pintavirooj and M. Sangworasil
Department of Electronics, Faculty of Engineering, and
Research Center for Communications and Technology (ReCCIT)
King Mongkut's Institute of Technology Ladkrabang

Abstract: In order to render 3D model of the bone, the stack of cross-sectional images must be reconstructed from a series of X-ray radiographs, served as the projections. In the case where the distance between x-ray source and detector is not infinite, image reconstruction from projection based on parallel-beam geometry provides an error in the cross-sectional image. In such case, image reconstruction from projection based on conebeam geometry must be exercised instead. This paper is devoted to the determination of detector center for SART conebeam Technique which is critically effect the performance of the resulting 3D modeling.

Keywords: Image Reconstruction, Backprojection, SART, Volume Rendering, Radiograph

1. INTRODUCTION

Three-dimensional (3D) visualization, including surface rendering and volume rendering, has been studied extensively for medical application for the past several years and applied to such various medical applications as volume measurement, surgical planning, automated image-guided surgery, and telepresence surgery. The 3D visualizations are well established as clinical tool for CT imaging [1-2]. Visualization techniques for MRI and PET have been explored in [3-4]. Recently, special techniques have been purposed for multi-modal image which is the combination of PET and MR data [5-6]. 3D-image reconstruction for 3D ultrasonic data has been investigated in [7-8] to visualize the left ventricle of heart and the mitral valve.

Recently, we have proposed the 3D visualization from X-ray radiographs by deriving the stack of cross section from the filtered backprojection technique (FBP) and Algebraic Reconstruction Technique (ART) [9-10]. In those researches, the 3D visualizations are consequently obtained from rendering the stack of cross-sectional images, so-called volumetric data, by the rendering technique. Hence, having high quality cross-sectional images is necessary as well. The scheme to inverse the projections to a cross section can be categorized into 2 classes, the transformation method [11] such as the FBP and the algebraic formulation [12] such as the ART. It is proved by [13] that, for the same limited number of projections, the algebraic formulation gives the better result of cross section than that of the transformation method. We have shown that the algebraic reconstruction is suitable for the X-ray radiography which has limited projections caused by the X-ray overdose problem.

Image reconstruction from projection used in [9], [10] and [15] is based on the assumption that the beam geometry is parallel. In practice, however, the assumption is acceptable only in the case where the distance between x-ray source and film (or detector) is relatively high. If this is not the case i.e. for (C-ARM x-ray Apparatus), conebeam geometry must be applied. The implementation of conebeam -geometry reconstruction algorithm, however, requires that the center location of the detector is accurately identified. Any slightly-missed alignment of the x-ray soure or the detector could result in the error of the position of the center and hence the error in reconstructed image. The aim of this paper is to the determination of detector center for SART conebeam technique.

This paper is structured as the following. Section 2 explains for detector-center determination succeeding section is for simulation results on the phantom model followed by the practical results tested on a series of X-ray radiographs of the human femur bone. Conclusions and Discussion is provided in the last section.

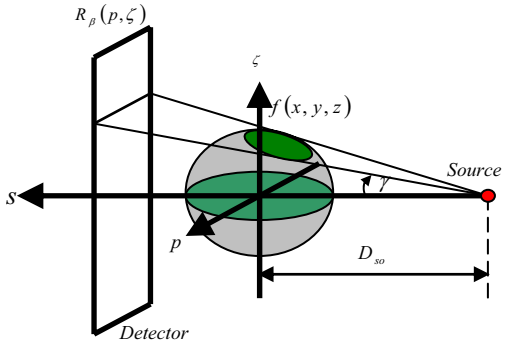

Fig. 1 Cone Beam Geometry.

2. DETECTOR-CENTER DETERMINATION

The implementation of SART conebeam (shown in figure 1) requires that the center location of the detector or $R_\beta(p, \zeta)$ is accurate. Any slightly-missed alignment of the x-ray soure or the detector could result in the error of the position of the center. This section is devoted to the determination of detector center. The procedure is performed by taking the radiograph of the square-metal tube. The shadow-gram of the tube is then analyzed to determine the center location.

In Fig.3, (a) is an x-ray radiograph of the box model from a C-Arm x-ray apparatus that is demonstrated the conebeam by shade of the object in Fig. 3. (b) (Top view). Size of the azimuth object show on a scene that is presented by A_o = 4.5 cm and B_o = 4.5 cm. For A_s and B_s are the size of shade, it is to exceed more than the object's size because it is indicated to the conebeam. When the center of rotation of point source is placed on the center of the object, both side (Δs_{l1} and Δs_{r1}) of shade will equally. We is written relation as

$$tan(\psi_1) = \frac{\Delta sl_1}{L_1} \quad (1)$$

$$tan(\psi_1) = \frac{\Delta sl_2}{L_2} \quad (2)$$

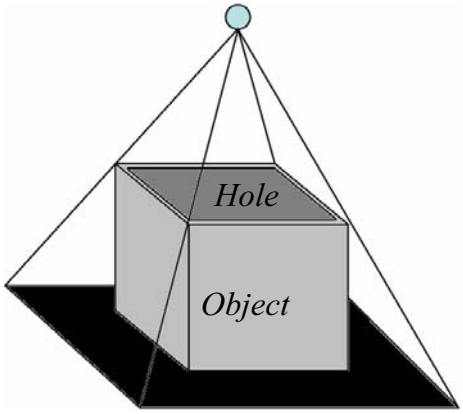

(a)

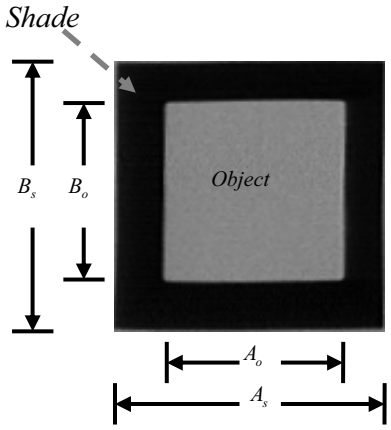

(b)
Fig. 3

$$tan(\psi_2) = \frac{\Delta sr_1}{L_1} \tag{3}$$

$$tan(\psi_2) = \frac{\Delta sr_2}{L_2} \tag{4}$$

$$\frac{\Delta sl_1}{\Delta sl_2} = \frac{L_1}{L_2} \tag{5}$$

$$\frac{\Delta sr_1}{\Delta sr_2} = \frac{L_1}{L_2} \tag{6}$$

$$A_o = \Delta sl_2 + \Delta sr_2 \tag{7}$$

$$A_s = \Delta sl_1 + A_o + \Delta sr_1 \tag{8}$$

ψ_1 and ψ_2 is the inner angles of rays touch the top corner of box show that the relation of length from the point source to scene show in Fig. 4(b). The distance from edges of the box and shade to center rotation are Δs_{l1}, Δs_{l2},Δs_{r1} and Δs_{r2}. The altitude of box is L_1 and distance from top of box to point source is L_2. Length of box A_o explained by Δs_{l2} and Δs_{r2}, A_o can be obtained from the summation of Δs_{l1}, ΔA_o and Δs_{r1}. When the point source is shifted that shown in Fig. 4(a), we can be written as

$$tan(\psi_1') = \frac{\Delta sl_1'}{L_1} \tag{9}$$

$$tan(\psi_1') = \frac{\Delta sl_2'}{L_2} \tag{10}$$

$$tan(\psi_2') = \frac{\Delta sr_1'}{L_1} \tag{11}$$

$$tan(\psi_2') = \frac{\Delta sr_2'}{L_2} \tag{12}$$

$$\frac{\Delta sl_1'}{\Delta sl_2'} = \frac{L_1}{L_2} \tag{13}$$

$$\frac{\Delta sr_1'}{\Delta sr_2'} = \frac{L_1}{L_2} \tag{14}$$

$$m = \frac{L_1}{L_2} \tag{15}$$

$$A_o = \Delta sl_2' + \Delta sr_2' \tag{16}$$

$$A_s' = \Delta sl_1' + A_o + \Delta sr_1' \tag{17}$$

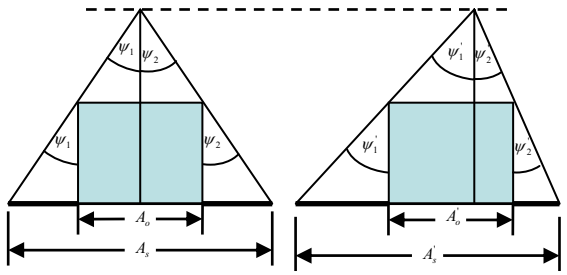

(a)

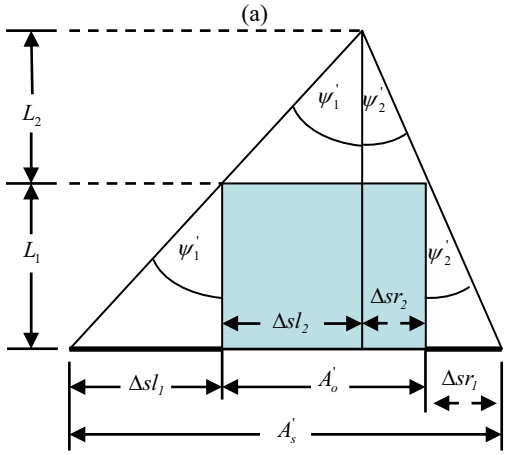

(b)
Fig. 4.

The stretch of shaded A_s and A_s' are equally distance, we show that by

$$
\begin{aligned}
A_s &= \Delta sl_1 + A_o + \Delta sr_1 \\
&= m \cdot \Delta sl_2 + m \cdot \Delta sr_2 \\
&= (m+1) \cdot A_o
\end{aligned} \tag{18}
$$

$$
\begin{aligned}
A_s' &= \Delta sl_1' + A_o + \Delta sr_1' \\
&= m \cdot \Delta sl_2' + m \cdot \Delta sr_2' \\
&= (m+1) \cdot A_o
\end{aligned} \tag{19}
$$

In this problem, we need to found Δs_{l2}' and Δs_{r2}'when know A_o, A_s, Δs_{l1}', Δs_{r1}' and L_1. First, we suppose Δs_{l1}, Δs_{l2}, Δs_{r1} and Δs_{r2}, those can be obtained the other parameters such as L_1 in (15) or (16) then Δs_{l2}' and Δs_{r2}' is obtained by (23) and (24). For this, A_s = 4.5 cm, A_o = 4.5 cm, B_s = 4.5 cm, B_o = 4.5 cm, Δs_{l1}' = 1.2375 cm, Δs_{r1}' = 1.0125 cm and L_1 = 30.6 cm, Δs_{l2}' is 2.475 cm and Δs_{r2}' is 2.025 cm. The other side we are solved from B_o and B_s which the results are shown center of the point source in Fig. 5.

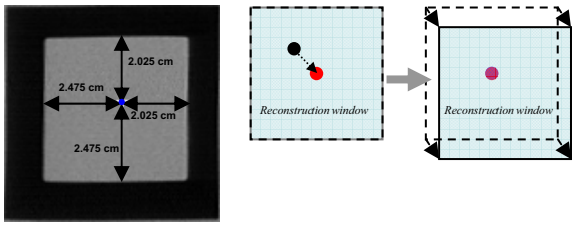

Fig. 5.

3. 3D RECONSTRUCTION FOR C-ARM X-RAY APPARATUS

The complement of this paper is to reconstruct the stack of cross-sectional images from the radiographs of Femur Bone, and to display it as a 3D model by the volume-rendering technique. To collect the radiographs, we have used BV-29 Phillips C-ARM X-ray apparatus. The apparatus is capable of providing a digital-form radiograph and information about the collected angle. The tested phantom is a human femur bone. The number of projection is 36 or 5 degrees per radiograph from 0 to 180°. Figure 6 shows an example of radiographs of femur. These radiographs served as a 2D projection data for SART conebeam

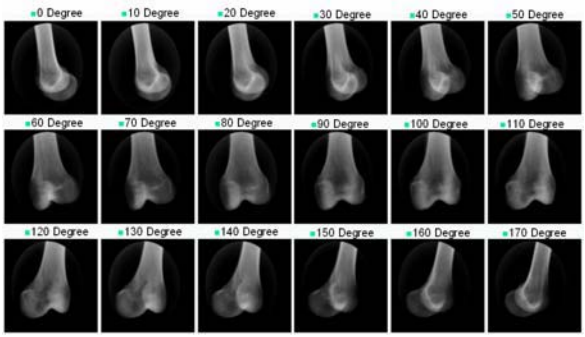

Fig. 6 Sample of X-ray radiographs taken from 60 angles in the half plane.

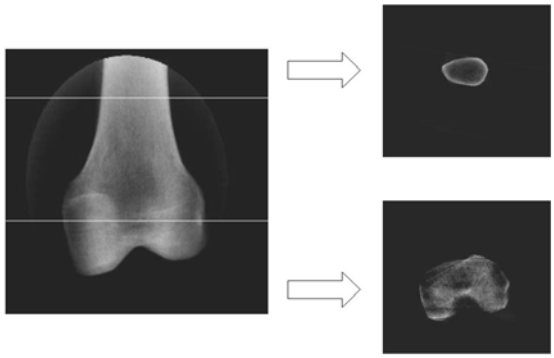

Fig. 7 The cross sections of femur bone reconstructed by the SART conebeam.

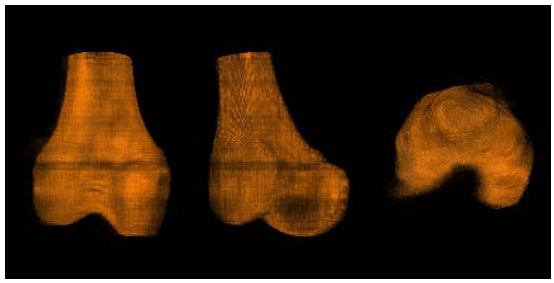

Fig. 8 Three views of the volume rendering of human femur bone

The projected data used for the image reconstruction is extracted from each of the horizontal line of the digitized image. Figure 7 shows sample of reconstructed images using SART conebeam. After the reconstruction processes, all of the slices is stacked to form the volumetric data. The volume rendering is then performed on the stacks of data to provide a 3D visualization. After adding the lighting model for more reality, the 3D visualizations are available as shown in Figure 8.

4. CONCLUSIONS

The application of image reconstruction from projection based on cone-beam geometry is implemented in this paper. The center for conebeam Technique is critically effects the performance of the resulting 3D modeling. In this paper, we focus on the center determination for conebeam x-ray tomography by analyzing the radiograph of the square-metal tube. The qualities of cross-sectional images and the resulted 3D model of Human femur bone from SART conebeam algorithm is improved after the center of the accurately identified.

REFERENCES

[1] D.C. Hemmy, et. al., "Three-dimensional Reconstruction of Craniofacial Deformation using Computed Tomographic," *Neurosurgery*, vol. 13, pp. 534-541, 1983.

[2] W.G. Totty, and N.W. Vannier, "Analysis of Complex Masculoskeleton Anatomy using Three-dimensional Surface Reconstruction," *Radiology*, vol. 150, pp. 173-177, 1984.

[3] L. Axel, et. al., "Three-dimensional Display of NMR Cardiovascular Images," *Comput. Assist. Tomography*, vol.7, pp. 172-174, 1983.

[4] N.W. Vannier, et. al., "Three-dimensional Magnetic Resonance Imaging of Congenital Heart Diseases," *Radiographics*, vol. 8, no. 5, pp. 857-871, 1988.
[5] D.N. Levin, et. al., "Integrated Three-dimensional Display of MR and PET Images of the Brain," *Radiology*, vol. 172, pp. 783-789, 1989.
[6] N.J. Valentino, "Volume Rendering of Multimodal Image: Application of MRI and PET image of the Human Brain," *IEEE Trans. Medical Imaging*, vol. 10, no. 4, pp. 554-561, 1991.
[7] R. Pini, et. al., "Echocardiographic Three-dimensional Visualization of the Heart," *NATO ASI Series*, vol. F60, 3D imaging in Medicine, Hohne, K. H. et. al., Eds., Berlin: Springer-Verlag, 1990.
[8] M. Verlande, et. al., "3D Reconstruction of the Beating Left Ventricle and Mitral Valve based on Multiplanar tee," in *Proc. Computers in Cardiology*. New York: IEEE Computer Society Press, 1991.
[9] C. Pintavirooj, C. Ninkaew, M. Sangworasil, and K. Hamamoto, "3D Visualization from Radiograph," *ISCIT2001*, pp. 307-310, Nov. 2001.
[10] P. Ungpinitpong, C. Pintavirooj, P. Leartprasert, and M. Sangworasil, "Improved 3D Visualization from X-Ray Radiograph Using Algebraic Reconstruction Technique," *ISCIT2002*, Oct. 2002.
[11] A.C. Kak, "Tomographic Imaging with Diffracting and Non-Diffracting Sources," *Array Signal Processing*, S. Haykin, Ed. Eaglewood Cliffs, NJ: Prentice-Hall, 1985.
[12] S. Kaczmarz, "Angenaherte Auflosung Von Systemen Linearer Gleichungen," *Bull. Acad. Pol. Sci. Lett. A*, vol. 6-8A, pp. 355-357, 1937.
[13] H. Guan, and R. Gordon, "Computed Tomography using Algebraic Reconstruction Techniques (ART) with Different Projection Access Schemes: A Comparison Study Under Practical Situations," *Phys. Med. Biol.*, No.41, pp.1727-1746, 1996.
[14] A.C. Kak, and M. Slaney, "*Princicles of Computerized Tomographic Imaging,*" IEEE Press, NY, 1988.
[15] P. Ungpinitpong, S. Ngamanekrat, C. Pintavirooj and M. Sangworasilp, "SART: AN APPROACH TO IMPROVE 3D VISUALIZATION FROM LIMITED VIEWS OF X-RAY RADIOGRAPHS", World Congress on Medical Physics and Biomedical Engineeering (WC2003), Sydneys, Australia, August 2003.